

Continuous-wave 355-nm laser source based on doubly resonant sum-frequency mixing in an external resonator

Yushi Kaneda and Shigeo Kubota

Kubota Opto-Electronics Laboratory, Sony Research Center, 6-7-35 Kitashinagawa, Shinagawa-ku, Tokyo 141, Japan

Received June 9, 1995

Using doubly resonant sum-frequency mixing between 1064 and 532 nm in an external resonator, we obtained 186 mW of continuous-wave ultraviolet output at $\lambda = 355$ nm with more than 20% conversion efficiency from the total incident power onto the mixing cavity. The resonator mirrors are shared by both the 1064- and the 532-nm beams, yielding an optimum mode overlap between the two resonating modes. To maintain the simultaneous resonance, we locked the external resonator to the single-frequency green laser and locked the 1064-nm laser to the resonator. This technique can be applied to cw sum- or difference-frequency mixing of any two wavelengths. © 1995 Optical Society of America

Continuous-wave ultraviolet sources near 350 nm are attractive for applications including the mastering of optical disks as replacements for UV argon-ion lasers. By third-harmonic generation of Nd lasers near 1064 nm, 355-nm output can be obtained. To obtain 355-nm output, one must mix two beams at 532 and 1064 nm, both of which are available in cw mode with current technology.

So far, resonant second-harmonic generation, or, in other words, doubly resonant sum-frequency mixing (DRSFM) between the same wavelengths, has been demonstrated with excellent conversion efficiencies into green light.¹⁻³ Cw DRSFM of two different wavelengths to the UV region in an external resonator has been demonstrated with 31 μ W of output power.⁴ Also, one can find some demonstrations of DRSFM in the blue region (459–462 nm) in a coupled laser cavity⁵ or in an external resonator.⁶

In this Letter we report a cw diode-pumped all-solid-state 355-nm laser source with an output power close to 200 mW, based on DRSFM in an external resonator. The conversion efficiency was enhanced by the high intensity of the circulating field in the external resonator.

In a sum-frequency-mixing process the output is proportional to the product of the powers at two input frequencies in the nondepleted approximation, which is valid for cw operation at power levels of 1 W or less. The output at the sum frequency is expressed as

$$P_{\text{SFG}} = \gamma_{\text{SFG}} P_{c1} P_{c2}, \quad (1)$$

where P_{c1} and P_{c2} represent the optical powers incident upon the nonlinear crystal at frequencies ω_1 and ω_2 , respectively, and γ_{SFG} represents the normalized conversion efficiency.⁷ In the case of 355-nm generation the choice of the nonlinear crystal is limited to a few candidates owing to their transmission cut-off and phase-matching conditions. For most of the available nonlinear materials, including beta-barium metaborate (BBO), γ_{SFG} is typically on the order of 10^{-5} – 10^{-4} W^{-1} , so one would need an input power of

30 W at each input frequency (60 W in total) to obtain an output power of the order of 0.1 W. In the resonant conversion configuration, in which the input powers are enhanced by the resonance, the incident powers to the nonlinear crystal are

$$P_{c1} = E_1 P_{i1}, \quad (2a)$$

$$P_{c2} = E_2 P_{i2}, \quad (2b)$$

where P_{i1} and P_{i2} are the optical powers that are coupled to the resonator and E_1 and E_2 are the enhancement factors at frequencies ω_1 and ω_2 , respectively. Substituting Eqs. (2a) and (2b) into Eq. (1), we obtain

$$P_{\text{SFG}} = \gamma_{\text{SFG}} E_1 E_2 P_{i1} P_{i2}, \quad (3)$$

indicating $E_1 E_2$ times enhancement of the total conversion efficiency over the single-pass conversion efficiency. An enhancement factor of approximately 100 can be obtained when the resonator has a finesse of ~ 300 . When the finesse for each frequency is ~ 300 , the total sum-frequency conversion efficiency can be enhanced by a factor of $\sim 100^2 = 10,000$. This yields a total conversion efficiency on the order of 1 W^{-1} , meaning 0.1–0.2-W generation from incident powers of less than 1 W at each frequency. In the case of singly resonant conversion, one of the enhancement factors becomes unity, reducing the total conversion efficiency to an impractical value. Therefore resonating the inputs at both frequencies is necessary at power levels at or below 1 W.

A schematic of the experimental setup is shown in Fig. 1. The DRSFM resonator resonates at both 532 and 1064 nm and has a bow-tie design consisting of two flat mirrors and two 30-mm concave mirrors, one of which is the input/output coupler, and a 3-mm-long BBO crystal. One of the flat mirrors is mounted on a voice coil motor (VCM),⁸ which is an electromagnetic precision-positioning device that provides control of the

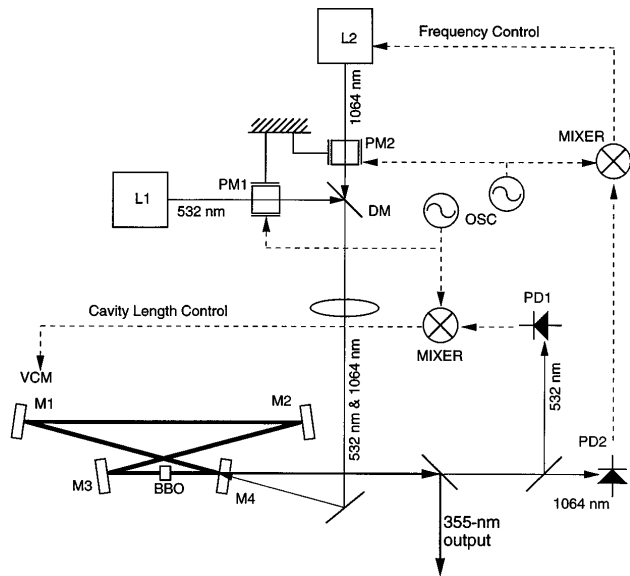


Fig. 1. Schematic of DRSFM: L1, laser 1 (532 nm); L2, laser 2 (1064 nm); PM1, PM2, phase modulators; DM, dichroic mirror; OSC, oscillators; PD1, PD2, photodiodes; M1–M3, dual high-reflection mirrors; M4, dual input/output mirror. Solid lines represent the optical path, and dashed lines represent the flow of the servo loops.

cavity length. M1, M2, and M3 are high reflectors for both 532 and 1064 nm (dual high-reflection mirrors), and M4 is the dual input coupler, which has $\sim 99\%$ reflectivity at 532 nm, $\sim 99.3\%$ reflectivity at 1064 nm, and $\sim 90\%$ transmission at 355 nm and serves as the output mirror as well. These reflectivities yield impedance matching when the sum of the passive loss and the nonlinear depletion equals the transmission of the input coupler, hence producing good coupling efficiency of the inputs into the external resonator. We anticipated well below 1% single-pass nonlinear depletion and less than 1% passive loss; therefore $\sim 99\%$ reflectivities are close to the optimum in terms of impedance matching. Both faces of the BBO crystal are antireflection coated at both 532 and 1064 nm (dual antireflection coating). In this configuration the modes are defined only by one set of mirrors. Assuming that the dispersion of the resonator at the two input wavelengths have identical spatial distributions, except that the mode sizes differ by the factor of the ratio of the square root of the wavelengths. This yields the identical focusing parameter for both modes, and hence the mode overlap at the nonlinear crystal is maintained at the optimum. Therefore this design significantly reduces the difficulty in the alignment procedure since mode matching is required only between the input beams and the resonator eigenmode. With two 30-mm radius-of-curvature mirrors the eigenmode radius sizes are approximately 15 and 20 μm at 532 and 1064 nm, respectively. The loss of the resonator, excluding the loss that is due to the sum-frequency-mixing process, is estimated from the finesse to be approximately 0.5% for both wavelengths. We performed this measurement by scanning the cavity or the laser frequency in the absence of the other

input, hence eliminating the sum-frequency-mixing process. To maintain the low loss of the resonator, we place no other element in the cavity. Therefore the resonator does not have dispersion tuning capability, although it is capable of tuning the resonance frequency, and one of the two laser sources needs to be frequency tunable by as much as the free spectral range of the DRSFM cavity, which is approximately 1.3 GHz. The full range of the free spectral range is not required for fast tuning, but fast-frequency tunability is required to follow the frequency jitter of the DRSFM cavity, which reflects the frequency jitter of the laser that the DRSFM cavity is locked to.

The green (532-nm) source used in this experiment is a diode-pumped intracavity-doubled Nd:YVO₄ laser oscillating in single frequency. The single-frequency output is obtained by a laser head similar to what is described in Ref. 9 (see Fig. 2). We maintain stable single-frequency operation, confirmed from the reflection dip from the external cavity while it is scanned, by tuning the temperature of the KTP crystal. This crystal is placed at the tightly focused waist of the laser resonator and forms a birefringent filter with the Brewster window in the cavity and the polarization-dependent gain of the Nd:YVO₄ laser crystal. The laser head is pumped with a fiber-coupled 10-W AlGaAs laser diode (Spectra Diode Laboratories, SDL-3450-P5), producing as much as 940 mW of power at 532 nm with an incident pump power of 8.5 W. The green laser is free running and does not have the frequency tuning capability.

The 1064-nm source is a tunable Nd:YVO₄ laser consisting of a 2-at.% 0.5-mm-long Nd:YVO₄ laser crystal and a 250-nm radius-of-curvature concave 5% output coupler, which is mounted on a VCM. The 1064-nm source has an output power of typically more than 350 mW when end pumped with a 1-W broad-area AlGaAs diode laser. The output spectrum consists

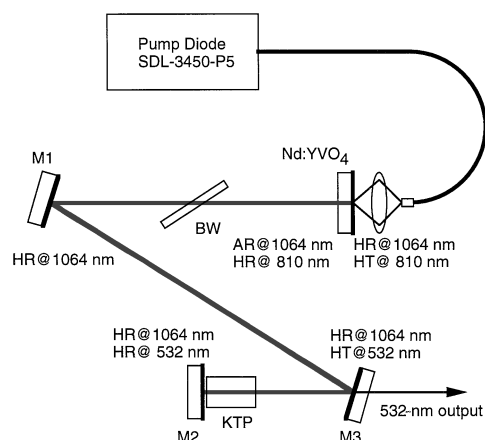


Fig. 2. Schematic of laser 1: BW, Brewster window; HR, highly reflective; AR, antireflective; HT, highly transmissive. The c axis of the Nd:YVO₄ crystal and the p polarization of the Brewster window are in the plane of the page. The z axis of the KTP crystal is oriented 45° with respect to the plane of the page, forming a birefringent filter with the Brewster window and the polarization-dependent gain of Nd:YVO₄. The birefringent filter acts as the frequency-selection component.

of typically two frequency components, one of which contains $\sim 70\%$ of the power and is locked and coupled to the external cavity. The 1064-nm laser frequency can be tuned by the VCM, with a tuning rate of more than 20 GHz/s, and the laser can be locked to the external cavity while the external cavity is scanned by more than two free spectral ranges every $1/10$ s. Improvement in the sum-frequency output power should be possible by single-frequency operation, thus increasing the input power that is coupled to the external cavity.

Two input beams are modulated in phase at 20 MHz, which is well above the resonance width of the resonator, and then combined with the same focusing parameter by use of a dichroic mirror before incidence on the mixing resonator. After the coupling optics the incident powers onto the mixing resonator are 670 and 280 mW at 532 and 1064 nm, respectively, yielding a total incident power of 950 mW. The locking servo loops employ the Pound–Drever–Hall technique.¹⁰ In the present setup, two separate modulators and two separate detectors are used for the two servo loops, along with wavelength-discriminating filters, completely separating the two servo loops, with no cross talk.

The resonator length is adjusted with the VCM. The external cavity is locked to the green source since the green source is not frequency tunable. After locking the resonance of the cavity to the green light we lock the frequency of the 1064-nm laser to the cavity by controlling the oscillation frequency with the VCM, thereby providing the double resonance. A 532-nm laser source and a 1064-nm laser source were used in this experiment; however, this DRSFM technique is essentially applicable to cw sum- and difference-frequency mixing of any combination of wavelengths.

When the two fundamental beams are both at resonance, the circulating powers in the resonator are approximately 70 and 20 W. We detected an output power of 186 mW at 355 nm outside the cavity, indicating the generation of more than 200 mW of power, taking into account the transmission of output mirror M4. This result indicates a total conversion efficiency of more than $200 \text{ mW}/(670 \text{ mW} + 280 \text{ mW}) = 20\%$. The nonlinear loss of the resonator, i.e., the single-pass nonlinear depletion of the input, is estimated to be 0.2%–0.3%, indicating good impedance matching. Theory predicts the normalized conversion efficiency γ_{SFG} for the experimental parameters to be approximately $1.5 \times 10^{-4} \text{ W}^{-1}$, yielding an output power of 210 mW, which is in good agreement with the experiment. Further improvement in the total conversion efficiency should be possible by means of the reduction of the loss in the external resonator.

The resonator modes of the two input waves are defined by the four resonator mirrors, yielding waist sizes proportional to the square root of the wave-

lengths. Therefore the output at 355 nm also has essentially the same focusing parameter, except that the beam is affected by the walk-off in one direction. A BBO crystal cut at $\theta = 31.3^\circ$ has 4.1° (7.2 mrad) of walk-off, producing a near-top-hat-shaped near-field pattern at the exit face of the BBO crystal. Hence the far-field pattern is diffraction limited in the non-walk-off direction and resembles a sinc^2 function in the walk-off direction, which is the Fourier transform of a top-hat pattern and can be compensated for by use of cylindrical optics or anamorphic prisms.

In conclusion, we have demonstrated 186 mW of 355-nm cw output from a diode-pumped solid-state laser source based on doubly resonant sum-frequency mixing in an external resonator, with more than 20% conversion efficiency from the total incident power onto the mixing cavity. The external resonator is formed with dual-wavelength mirrors, yielding optimum mode overlap between two input modes. This configuration can be applied to cw sum- and difference-frequency mixing of any combination of wavelengths.

The authors gratefully acknowledge technical support from Naoya Eguchi, Tsutomu Okamoto, Nobuhiko Umezumi, Minehiro Tonosaki, Hiroyuki Wada, and Yasujiro Taguchi of the Kubota Opto-Electronics Laboratory, Sony Research Center, and fruitful and interesting discussions with Robert L. Byer and Martin M. Fejer of Stanford University.

References

1. W. J. Kozlovsky, C. D. Nabors, and R. L. Byer, *IEEE J. Quantum Electron.* **24**, 913 (1988).
2. Z. Y. Ou, S. F. Pereira, E. S. Polzik, and H. J. Kimble, *Opt. Lett.* **17**, 640 (1992).
3. L. Y. Liu, M. Oka, W. Wiechmann, and S. Kubota, *Opt. Lett.* **19**, 189 (1994).
4. M. Watanabe, K. Hayasaka, H. Imajo, R. Ohmukai, and S. Urabe, *Jpn. J. Appl. Phys.* **33**, 1599 (1994).
5. R. Scheps and J. F. Myers, *IEEE J. Quantum Electron.* **30**, 1050 (1994).
6. W. P. Risk and W. J. Kozlovsky, *Opt. Lett.* **17**, 707 (1992).
7. G. D. Boyd and D. A. Kleinman, *J. Appl. Phys.* **39**, 3597 (1968).
8. M. Oka, N. Eguchi, L. Y. Liu, W. Wiechmann, and S. Kubota, in *Conference on Lasers and Electro-Optics*, Vol. 8 of 1994 OSA Technical Digest Series (Optical Society of America, Washington, D.C., 1994), paper CThM1.
9. W. Weichmann, L. Y. Liu, and S. Kubota, in *Advanced Solid-State Lasers*, Vol. 24 of OSA Proceedings Series, B. Chai and S. Payne, eds. (Optical Society of America, Washington, D.C., 1995), paper WD4.
10. R. W. P. Drever, J. L. Hall, F. V. Kowalski, J. Hough, G. M. Ford, A. J. Munley, and H. Ward, *Appl. Phys.* **B** **31**, 97 (1983).